al., Eds. (Wiley, New York, 1999), unit 5.6. The RPCI-98 BAC library was gridded on positively charged nylon filters. Each clone was spotted in duplicate, and the entire library was represented on each 22 cm by 22 cm filter. An anchor clone (*Caenorhabditis briggsae* clone RPCI-94 1A1) was included at multiple locations in the grid to facilitate alignment. Overlapping oligonucleotide probes (double-stranded 40-nucleotide oligomers) were designed with a Perl script provided by J. McPherson. Probe design was restricted to sequences with an average PHRED quality score of >q10 (*29*) unless sequence trace files were not available. Each ^{32}P-labeled probe was hybridized along with the anchor clone probe (GTTGCCAAATTCCGAGATCTTGGCGACGAAGCCACATGAT) to a separate filter. Filter images were collected on a PhosphorImager (Storm 860, Molecular Dynamics, Sunnyvale, CA) and analyzed in the ArrayVision module of the software package AIS v5.0 (Imaging Research, St. Catharines, Ontario, Canada) with the anchor signals for alignment. Filters were stripped and reused several times.

11. E. D. Green and P. Green, *PCR Methods Appl.* **1**, 77 (1991). Information on SEGMAP is available at www.genome.washington.edu/uwgc/analysistools/segmap.htm. Perl scripts were written to organize the STS content data (AIS output) by chromosome arm and export it to the individual SEGMAP projects. The scripts allowed an editor to move markers between chromosome arms or remove them entirely. Each data file contained only BACs hybridizing to the current probe because BACs corresponding to the previous hybridization experiment for the same filter were subtracted from it.
12. A false negative rate of 5% was calculated as the fraction of probes designed from BAC end sequences that failed to hybridize to their source BAC. A false positive rate of 8% was estimated as follows: For each BAC with multiple locations in the map, we designated all STS hits except those at the most likely location to be false positives; the most likely map location was deemed the one with the most consecutive STS hits. We then divided the total number of false positive hits by the total number of hits in the complete data set to arrive at the false positive rate. We also calculated that 81% of BACs contained neither a single false negative nor a false positive.
13. Web fig. 1 (*30*) shows a sample region of the STS content map in the SEGMAP display format. The edited STS content maps were reformatted and displayed on the World Wide Web (*5*) by means of custom Java tools. This public version excludes BACs with an inferred false positive hit or more than one inferred false negative hit, unless such BACs are part of the sequenced tiling path.
14. The *D. melanogaster* BAC (Dros BAC) library was made by A. Billaud for the European *Drosophila* Genome Project from DNA prepared from embryos of the isogenic y^1; cn^1 bw^1 sp^1 strain (*6*), partially digested with either Nde II or Hin DIII, and cloned in pBeloBAC11. Filters representing the 23,400 BACs in the library were hybridized and analyzed as described. Additional information on the Dros BAC library is available at www.hgmp.mrc.ac.uk/Biology/descriptions/dros_bac.html.
15. M. A. Marra *et al.*, *Genome Res.* **7**, 1072 (1997). Restriction fingerprints were generated as described with the following modifications: For consistent growth, duplicate 1.2-ml cultures in 96-well format were inoculated with 50 μl of saturated starter culture and grown overnight. The pooled bacterial pellets were resuspended in 200 μl of GET buffer [25 mM tris-Cl (pH 8.0), 10 mM EDTA, and 150 mM glucose] supplemented with ribonuclease A (0.2 mg/ml) and lysozyme (2 mg/ml) before addition of 400 μl of 0.2 M NaOH/1% SDS and 300 μl of 3 M KOAc (pH 5.5). Lysates were vacuum-filtered (Qiagen Qiafilter or Polyfiltronics 0.45-μm polyvinylidene difluoride filter plates), and DNA was precipitated by the addition of 700 μl of isopropanol. Samples were resuspended in 20 μl of 10 mM tris-Cl (pH 8.0)/0.1 mM EDTA and digested (5 μl) in 10-μl Eco RI reactions. After digestion, 2 μl of loading dye supplemented with 0.1% SDS was added, and samples were heated to 65°C for 30 min and cooled on ice before loading on 1% agarose gels (Owl A2-BP gel boxes; custom 43-well combs). Molecular weight standards (1 Kb Extension Ladder, Life Technologies, Rockville, MD) were loaded in every sixth well, and electrophoresis was carried out at 70 V for 18 hours in TAE buffer (40 mM tris-acetate and 1 mM EDTA) recirculated at 12°C.
16. J. Sulston *et al.*, *Comput. Appl. Biosci.* **4**, 125 (1988). For a description of IMAGE, see www.sanger.ac.uk/Software/Image. Gel images were captured with a Molecular Dynamics FluorImager 595, and Perl scripts were written to organize image files for FPC assembly.
17. C. Soderlund, I. Longden, R. Mott, *Comput. Appl. Biosci.* **13**, 523 (1997).
18. Information on FPC is available at www.sanger.ac.uk/Software/fpc.
19. M. Ashburner *et al.*, *Genetics* **153**, 179 (1999).
20. FPC assembly of chromosome arm 3L was conducted at high stringency: a fixed tolerance of 6 and a cutoff setting of e^{-10} with equation 1 in (*17*). The finished sequence of the 2.9-Mb *Adh* region (*19*) was used to assess the accuracy of fingerprint assemblies at various FPC tolerance and cutoff settings, and a lower stringency was chosen for assembly of the 5-Mb projects: a fixed tolerance of 9 and a cutoff setting of e^{-6}.
21. See information at www.hgsc.bcm.tmc.edu/drosophila/mapping. As described by Marra *et al.* (*25*), the line drawings representing the fingerprint contigs may not accurately reflect the extent of BAC overlaps. Therefore, users should examine the IMAGE-processed gel lanes to verify BAC overlap; all files necessary for reassembly in FPC and fingerprint analysis are available. Web fig. 1 (*30*) shows STS content and restriction fingerprint assemblies in a sample region of the BAC map displayed in SEGMAP and FPC formats, respectively.
22. C. B. Bridges, *J. Hered.* **26**, 6 (1935).
23. V. Sorsa, *Chromosome Maps of Drosophila, Vol. II* (CRC Press, Boca Raton, FL, 1988).
24. T. Mozo *et al.*, *Nature Genet.* **22**, 271 (1999).
25. M. Marra *et al.*, *Nature Genet.* **22**, 265 (1999).
26. E. W. Myers *et al.*, *Science* **287**, 2196 (2000). Comparison of the order of STS markers in this BAC map and the whole-genome shotgun sequence assembly identified 10 discrepancies in STS location (>99.5% concordance), not including differences in local STS order that are due to the limited resolution of STS content mapping. Three of these STS markers appear to hybridize to duplicated sequences, and the other seven cases may result from duplicated sequences or data-tracking errors. We have removed all 10 from the public version of the STS content map to avoid potential confusion. BAC order and overlap were not substantially affected by these edits.
27. A. Peters *et al.*, unpublished material; available at www2.open.ac.uk/biology/molecular-genetics/EDGPMap.html.
28. J. Locke, L. Podemski, N. Aippersbach, H. Kemp, R. Hodgetts, *Genetics*, in press.
29. B. Ewing and P. Green, *Genome Res.* **8**, 186 (1998).
30. Web fig. 1 is available at www.sciencemag.org/feature/data/1048711.shl.
31. Instructions for preparing polytene chromosome in situ hybridizations are available at www.fruitfly.org/methods/cytogenetics.html.
32. We thank A. Gnirke for advice on preparation of HMW DNA; J. McPherson for "overgo" oligonucleotide probe labeling and hybridization protocols; R. Zhang, T. Wells, and C. Hamerski for technical support; A. Loraine for her work on the ArmView and CytoView Web displays; S. Mullaney for photography and assistance with figures; and B. Kimmel for discussions at the planning stage. We acknowledge Imaging Research for software improvements resulting in the release of AIS v5.0. Finally, we thank all members of the Berkeley *Drosophila* Genome Project and Human Genome Sequencing Center for their support. This work was supported by NIH grant HG00750 (to G.M.R.) and Howard Hughes Medical Institute (G.M.R. and T.R.L.).

18 January 2000; accepted 1 March 2000

Rapid Progression to AIDS in HIV$^+$ Individuals with a Structural Variant of the Chemokine Receptor CX_3CR1

Sophie Faure,[1] Laurence Meyer,[2] Dominique Costagliola,[3] Céline Vaneensberghe,[1] Emmanuelle Genin,[4] Brigitte Autran,[1] French ALT and IMMUNOCO Study Groups, Jean-François Delfraissy,[5] SEROCO Study Group, David H. McDermott,[6] Philip M. Murphy,[6] Patrice Debré,[1] Ioannis Théodorou,[1]* Christophe Combadière[1,6,7]

Human immunodeficiency virus (HIV) enters cells in vitro via CD4 and a coreceptor. Which of 15 known coreceptors are important in vivo is poorly defined but may be inferred from disease-modifying mutations, as for CCR5. Here two single nucleotide polymorphisms are described in Caucasians in CX_3CR1, an HIV coreceptor and leukocyte chemotactic/adhesion receptor for the chemokine fractalkine. HIV-infected patients homozygous for CX_3CR1-I249 M280, a variant haplotype affecting two amino acids (isoleucine-249 and methionine-280), progressed to AIDS more rapidly than those with other haplotypes. Functional CX_3CR1 analysis showed that fractalkine binding is reduced among patients homozygous for this particular haplotype. Thus, CX_3CR1-I249 M280 is a recessive genetic risk factor in HIV/AIDS.

The risk of HIV infection and the rate of HIV disease progression are both highly variable in populations, but factors responsible for this variability remain poorly defined. Mutations in genes for HIV-1 coreceptors and their natural chemokine ligands have been shown

to modify HIV-1 transmission and disease progression (*1*). The most powerful known cause of innate HIV resistance is CCR5Δ32, a mutant allele that encodes a truncated, inactive form of the chemokine receptor CCR5 (*2–7*). CCR5Δ32 heterozygosity does not restrict HIV infection but is associated with slower disease progression (*2, 4, 6, 7*), whereas CCR5Δ32 homozygotes are highly resistant to initial infection (*2–6*). Normally, CCR5 functions as a leukocyte chemotactic receptor but does not appear to be essential, or possibly even important, for immunocompetence as CCR5Δ32 homozygotes have no known health problems (*8*). A disease-accelerating allele has been found within the CCR5 promoter (59029-A allele or P1 haplotype), which may function by modulating CCR5 transcription (*9*).

Although powerful in their effects, these CCR5 variants account for only a small proportion of individuals with apparent HIV resistance; thus identification of other resistance factors remains an important aim in HIV research. A potentially related puzzle concerns the significance of the rest of the large and growing repertoire of HIV coreceptors, which to date includes 14 other chemokine receptors and related 7 transmembrane receptors (*10*). Each can support HIV entry at least to some extent by some strains in vitro, and cognate chemokine ligands can block this process. Several of these receptors have relatively restricted expression patterns, which suggests the possibility of compartment-restricted function in HIV infection. Moreover, all have defined or strongly suspected leukocyte chemoattractant activity and could alternatively or additionally be involved in the immune response to HIV. Thus, variation in expression or function of one or more of these genes also could contribute to disease heterogeneity. In this regard, variant alleles for the chemokine receptor/HIV coreceptor CCR2 (CCR2-64I allele) (*11*) and the chemokine receptor ligand SDF-1 (SDF1-3′A allele) (*12*) have been reported to be associated with slower HIV disease progression, although mechanisms have not been not established.

CX_3CR1, a leukocyte chemotactic and adhesion receptor for the chemokine fractalkine, is a recently identified HIV coreceptor (*13, 14*) expressed in many tissues but at particularly high levels in brain (*15*) and in interleukin-2-activated peripheral blood lymphocytes (*16*). CX_3CR1 interacts with a limited number of commonly tested HIV envelopes, and fractalkine can efficiently block the HIV coreceptor activity of CX_3CR1 (*14*). Interestingly, besides its chemotactic activity, fractalkine has unprecedented adhesion properties (*17*). When anchored to the membrane, it may play an important role in the immune response by reinforcing cell contact. To investigate whether CX_3CR1 may regulate HIV disease, we searched for genetic variants associated with altered disease outcome.

We screened the CX_3CR1 coding sequence for mutations in 78 random French Caucasian blood donors by means of a single-stranded conformation polymorphism (SSCP) technique (*18*), and we identified 5 single nucleotide polymorphisms (SNPs), all in transmembrane domains of the receptor. Four SNPs were nonsynonymous: (i) an A-to-G substitution changed Thr^{57} to Ala ($T^{57}A$), (ii) a G-to-A substitution changed Val^{122} to Ile (V122I), (iii) a G-to-A substitution changed Val^{249} to Ile (V249I), and (iv) a C-to-T substitution changed Thr^{280} to Met (T280M). The synonymous substitution was in codon 255 (G-to-A). Only T280M was nonconservative, exchanging a polar for a nonpolar side chain in the seventh transmembrane domain. The two SNPs in positions 57 and 122 were each found only once among 156 chromosomes, whereas the other nonsynonymous allelic variants, V249I and T280M, were quite common, 25.7% and 13.5%, respectively, in the uninfected population. These mutations appeared to be specific to the Caucasian population as they were not detected in populations of either Asian (92 chromosomes from Vietnamese donors) or West African (90 chromosomes) descent (*19*).

Using a restriction fragment length polymorphism–based method (*20*), we studied the distribution of V249I and T280M among 565 individuals from three HIV cohorts: patients with intermediate progression (IMMUNOCO cohort), patients with asymptomatic long-term progression (ALT cohort), and patients with a known date of seroconversion (SEROCO cohort) (*21*). Of the nine possible genotypes, six were observed (Table 1) at frequencies ranging from about 50% for the homozygous wild type to about 2% for the doubly mutated homozygote. Three genotypes were never detected: G/G at codon 249 followed by C/T at codon 280, G/G at codon 249 followed by T/T at codon 280, and G/A at codon 249 followed by T/T at codon 280. Their absence suggests the SNPs are tightly linked and probably the C/T substitution at position 280 occurred only when there was an A at codon 249. A likelihood ratio test for linkage equilibrium was performed and confirmed that these SNPs were in complete linkage disequilibrium ($D' = 0.999$; $P < 10^{-65}$). Therefore, only three haplotypes of CX_3CR1 were detected in the Caucasian population: the V249 T280 haplotype, the I249 T280 haplotype, and the I249 M280 haplotype (Table 1). Their respective frequencies in the Caucasian HIV-infected population were 71.4%, 12.4%, and 16.2% (*22*). There was no significant difference in observed haplotype frequencies between HIV-infected and uninfected individuals.

A departure from Hardy-Weinberg expectation was found for HIV-infected individuals for the CX_3CR1-T280M allele (21 individuals homozygous for T280 were observed versus 13 expected among 562 patients; $\chi^2 = 4.02$; $P < 0.045$), whereas no deviation was found in uninfected individuals ($P = 0.36$) (*23*). The deviation was even more pronounced in CCR5 wild-type HIV-infected individuals ($\chi^2 = 5.376$; $P < 0.021$). In contrast, neither CX_3CR1-V249I, CCR5-Δ32, nor CCR2-64I alleles showed a significant departure from Hardy-Weinberg expectation in HIV-infected or uninfected popula-

Table 1. Effects of CX_3CR1 variants on HIV pathogenesis. Frequencies of CX_3CR1 genotypes and haplotypes among the four French Caucasian cohorts examined in this study: asymptomatic long-term nonprogressors (ALT), standard progressors (IMMUNOCO), seroconverters (SEROCO), and uninfected blood donors. Values represent number of individuals in each category and values in parentheses represent percentage of individuals of each category in the whole cohort.

Genotype	V249I	T280M	ALT	IMMUNOCO	SEROCO	Uninfected
1	G/G	C/C	35 (55.5)	33 (45.2)	222 (52.1)	41 (52.6)
2	A/A	C/C	1 (1.6)	2 (2.7)	4 (0.9)	1 (1.3)
3	A/A	T/T	2 (3.2)	3 (4.1)	16 (3.8)	0 (0)
4	A/A	C/T	3 (4.8)	2 (2.7)	17 (4.0)	2 (2.6)
5	G/A	C/C	13 (20.6)	12 (16.4)	80 (18.8)	15 (19.2)
6	G/A	C/T	9 (14.3)	21 (28.8)	87 (20.4)	19 (24.3)
Total			63	73	426	78
Haplotype						
V249 T280	G	C	92 (73)	99 (67.8)	611 (71.7)	116 (74.3)
I249 T280	A	C	18 (14.2)	18 (12.3)	105 (12.3)	19 (12.2)
I249 M280	A	T	16 (12.6)	29 (19.8)	136 (16.0)	21 (13.5)
Total			126	146	852	156

[1]Laboratoire d'Immunologie Cellulaire et Tissulaire, Centre National de la Recherche Scientifique UMR 7627, Hôpital Pitié-Salpétrière, Paris, France. [2]Institut National de la Santé et de la Recherche Médicale U292, Département d'Epidémiologie, Hôpital de Bicêtre, Faculté de Médecine, Kremlin-Bicêtre, France. [3]Institut National de la Santé et de la Recherche Médicale SC4, Faculté de Médecine Saint-Antoine, Paris, France. [4]Institut National de la Santé et de la Recherche Médicale U155, Hôpital de Bicêtre, Kremlin-Bicêtre, France. [5]Service de Médecine Interne, Hôpital de Bicêtre, Kremlin-Bicêtre, France. [6]Laboratory of Host Defenses, National Institute of Allergy and Infectious Diseases, National Institutes of Health, Bethesda, MD 20892, USA. [7]Institut National de la Santé et de la Recherche Médicale U479, CHU Bichat, Paris, France.

*To whom correspondence should be addressed: E-mail: ioannis.theodorou@psl.ap-hop-paris.fr

tions ($P \sim 0.5$). These results suggest that the I249 M280 haplotype probably increases susceptibility to HIV infection. However, studies in other HIV cohorts are necessary to validate this hypothesis.

With respect to disease progression, a case control analysis showed a trend toward a higher frequency of the I249 M280 haplotype in the IMMUNOCO cohort compared with the ALT cohort [odds ratio (OR) = 2.1; 95% confidence interval (CI), 0.9–4.9; $P = 0.079$] (Table 2) (*24*). In contrast, the protective CCR5-Δ32 allele was more frequent in the ALT cohort (OR = 0.2; 95% CI, 0.1–0.5; $P = 0.0004$). These results suggest that the CX_3CR1 I249 M280 haplotype adversely affects HIV disease progression. Consistent with this, Kaplan–Meier survival analysis of seroconverters from the SEROCO cohort stratified by genotypes revealed faster progression to clinical AIDS for CX_3CR1-M280 homozygotes compared with CX_3CR1-T280 homozygotes [relative risk (RR) = 2.13; $P = 0.039$] (Fig. 1A). No significant effect was observed for CX_3CR1-V249I (*25*). The same conclusion can be drawn from Kaplan-Meier analysis of CD4 decline (RR = 1.96; $P = 0.08$), but only a trend toward significance (probably due to fewer events) was observed for time to death (RR = 1.84; $P = 0.18$). Disease progression was similar for heterozygotes and wild-type homozygotes. This suggests that the effect of the CX_3CR1-I249 M280 haplotype is recessive, in contrast to the CCR5-Δ32 and CCR2-64I alleles, which have dominant effects. The deleterious effect persisted after adjustment for age at seroconversion. Although the difference was no longer significant after adjustment for viral load (probably because of a reduced number of events, the viral load was available for only 350 of 426 patients), the tendency remained strong (RR = 2.00; $P = 0.131$), which suggests that this adverse deleterious effect was not mediated through a higher viral load. When patients partially protected by the CCR5-Δ32 allele were excluded from the analysis (Fig. 1B), the acceleration to AIDS (RR = 2.44; $P = 0.016$) or CD4 decline (RR = 2.55; $P = 0.017$) was more pronounced.

The CX_3CR1 gene is located on chromosome 3p21 in the vicinity of the CCR5 and CCR2 genes (*26*). Therefore, to verify that this effect can be attributed to CX_3CR1, we analyzed the CX_3CR1 SNP distribution in relation to the CCR5-Δ32 and CCR2-64I alleles. Neither CX_3CR1 SNP (V249I and T280M) exhibited linkage disequilibrium with either CCR2-64I (likelihood ratio test for linkage equilibrium, $P > 0.77$ and $P = 1.00$, respectively) or CCR5-Δ32 ($P > 0.79$ and $P > 0.55$, respectively). Furthermore, we observed no linkage disequilibrium between CX_3CR1 V249I and T280M and previously described SNPs in the CCR5 promoter region, including A29G, C927T, and A59029G (*9, 27*). Thus, the CX_3CR1-I249 M280 haplotype is independent of previously defined disease-modifying mutations in CCR5 and CCR2.

The two CX_3CR1 SNPs defining the CX_3CR1-I249 M280 haplotype are located in the coding sequence and therefore could directly affect receptor function. To test this, we compared fractalkine binding to primary peripheral blood mononuclear cells (PBMCs) (*28*) from HIV-infected patients homozygous for CX_3CR1-V249 T280 ($n = 4$) versus CX_3CR1-I249 M280 ($n = 4$) (Fig. 2). Scatchard regression analysis of the binding data revealed significantly reduced binding affinity of ^{125}I-labeled fractalkine to cells from CX_3CR1-I249 M280 homozygotes versus wild-type CX_3CR1-V249 T280 cells (12.2 ± 3.3 pM versus 37.1 ± 10.1 pM; $P = 0.033$), an indication that the two SNPs affect the integrity of the receptor. Further, the total number of binding sites per cell was dramatically reduced in CX_3CR1-I249 M280 homozygotes versus wild-type controls (432 ± 146 versus 2795 ± 1137 sites, respectively; $P = 0.033$). To resolve the specific effect on function of each SNP constituting the CX_3CR1-I249 M280 haplotype, we characterized fractalkine binding parameters for PBMCs from two patients homozygous for haplotype CX_3CR1-I249 T280. Receptor expression (1244 ± 339 sites per cell) was not significantly different from the other haplo-

Table 2. Predictive values of CX_3CR1 and CCR5 genotypes for IMMUNOCO status. Values in parentheses represent 95% CI); ORs are statistically significant if the CI values do not include 1.0. wt, CCR5 wild-type genotype; Δ32, deleted form of CCR5. Results are adjusted for age.

Genotype	ALT	IMMUNOCO	OR	95% CI	*P* value
CX_3CR1					
1+2+5	49	47	1		
3+4+6	14	26	2.1	(0.9–4.9)	0.079
CCR5					
wt	40	65	1		
wt/Δ32	23	8	0.2	(0.1–0.5)	0.0004

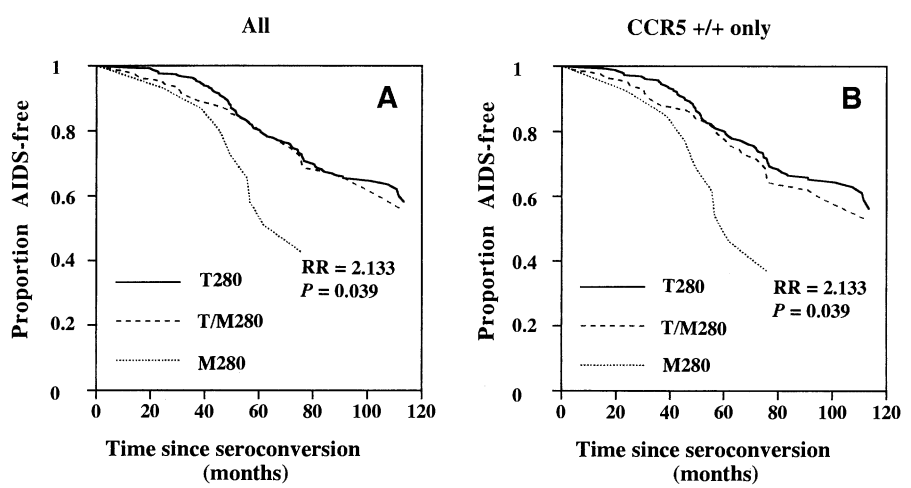

Fig. 1. Effect of CX_3CR1 variants on HIV disease progression. Time from seroconversion to clinical AIDS was examined in HIV-infected Caucasians from the SEROCO cohort. (**A**) Kaplan-Meier curves for the total SEROCO cohort (426 patients). (**B**) Kaplan-Meier curves for SEROCO patients homozygous for CCR5 wild type (356 patients).

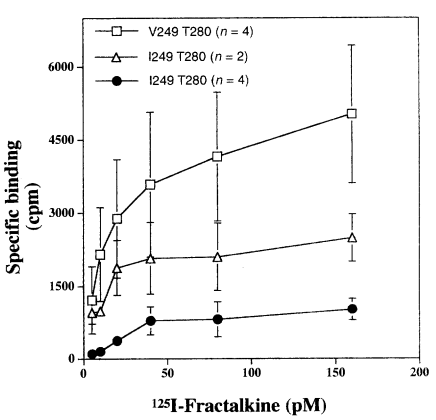

Fig. 2. Comparative analysis of fractalkine binding on PBMCs from homozygous patients with CX_3CR1 V249 T280 and I249 M280 haplotypes. Data represent specific binding in the presence of increasing amounts of iodinated fractalkine. Nonspecific binding (less than 10% of total binding) was subtracted from the total binding. Data are mean values ± SEM. Values in parentheses represent number of individuals in each category.

types tested; however, fractalkine binding affinity (4.5 ± 0.4 pM) differed ($P = 0.08$ and 0.02 for comparison with CX_3CR1-V249 T280 and CX_3CR1-I249 M280, respectively). These preliminary data suggest that T280M directly affects ligand recognition. Additional work is needed to know whether the effect on expression is due to modulation of synthesis, distribution or stability of receptor protein, or linkage with promoter alleles that modulate CX_3CR1 transcription.

Our results demonstrate that CX_3CR1 is polymorphic in the Caucasian population and that a particular variant haplotype, CX_3CR1-I249 M280, is associated with accelerated HIV disease. Potential mechanisms of action include regulation of HIV infection of target cells by CX_3CR1's HIV coreceptor activity and regulation of antiviral immune responses through cell recruitment and cell contact functions. CX_3CR1's HIV coreceptor activity is limited compared with CCR5 and CXCR4, which appear to account for cell entry of most HIV-1 strains in most primary cell types. However, there is precedent for use of at least one of the "minor" coreceptors in primary human cells, CCR3, which has been shown to operate in microglial cells of the central nervous system (*29*). The role of CX_3CR1 in these and other cell types of the nervous system where it is highly expressed is not known. Moreover, the strains used to test its HIV coreceptor activity have not included neurotropic isolates, which may be the most relevant in vivo.

If CX_3CR1 acts as an HIV coreceptor to modulate pathogenesis, then the accelerated progression noted in seroconvertors homozygous for CX_3CR1-I249 M280 could be explained by increased specific activity or an expanded strain range. The negative effects on fractalkine binding parameters found for this variant do not directly address this and may not be relevant because mutational analysis of other HIV coreceptors has revealed independent effects on HIV and chemokine binding parameters. Nevertheless, reduced receptor expression and fractalkine binding in itself could compromise normal immune responses, which might lead to accelerated progression. Additional work is under way to distinguish which of these mechanisms is responsible for the observed epidemiologic effects. However, because CX_3CR1 polymorphism is a risk factor in HIV disease and because CX_3CR1 is an HIV coreceptor, it is reasonable now to evaluate this receptor as a potential target for therapeutic intervention in HIV/AIDS.

References and Notes

1. R. Horuk, *Immunol. Today* **20**, 89 (1999); A. S. Fauci, *Nature* **384**, 529 (1996); J. S. Cairns and M. P. D'Souza, *Nat. Med.* **4**, 563 (1998).
2. M. Dean *et al.*, *Science* **273**, 1856 (1996); R. Liu *et al.*, *Cell* **86**, 367 (1996).
3. M. Samson *et al.*, *Nature* **382**, 722 (1996).
4. Y. Huang *et al.*, *Nat. Med.* **11**, 1240 (1996).
5. T. Dragic *et al.*, *Nature* **381**, 667 (1996).
6. P. A. Zimmerman *et al.*, *Mol. Med.* **3**, 23 (1997).
7. N. L. Michael *et al.*, *Nat. Med.* **3**, 338 (1997).
8. G. T. Nguyen *et al.*, *J. AIDS* **22**, 75 (1999).
9. D. H. McDermott *et al.*, *Lancet* **352**, 866 (1998); M. P. Martin *et al.*, *Science* **282**, 1907 (1998).
10. N. L. Michael, *Curr. Opin. Immunol.* **11**, 466 (1999); E. A. Berger *et al.*, *Annu. Rev. Immunol.* **17**, 657 (1999).
11. N. L. Michael *et al.*, *Nat. Med.* **3**, 1160 (1997); L. G. Kostrikis *et al.*, *Nat. Med.* **4**, 350 (1998); M. W. Smith *et al.*, *Science* **277**, 959 (1997).
12. C. Winkler *et al.*, *Science* **279**, 389 (1998).
13. J. Rucker *et al.*, *J. Virol.* **71**, 8999 (1997); J. D. Reeves *et al.*, *Virology* **231**, 130 (1997).
14. C. Combadiere *et al.*, *J. Biol. Chem.* **273**, 23799 (1998).
15. J. K. Harrison *et al.*, *Proc. Natl. Acad. Sci. U.S.A.* **95**, 10896 (1998); C. Combadiere *et al.*, *J. Leukocyte Biol.* **60**, 147 (1996).
16. T. Imai *et al.*, *Cell* **91**, 521 (1997).
17. A. M. Fong *et al.*, *J. Exp. Med.* **188**, 1413 (1998).
18. An initial screening for mutations in the CX_3CR1 coding sequence was done on about 100 North American random blood donors of mixed race by a directed heteroduplex technique described in (*6, 9*). This revealed the two common CX_3CR1 SNPs; V249I and T280M. Subsequently, a SSCP technique was used to confirm and extend this analysis. Amplification of a 1100–base pair (bp) fragment coding for the totality of receptor CX_3CR1, with two primers: V1 forward (5′-TACTTG TTTTTCTTTCTGATCCAGG-3′) and V5 reverse (5′-AGACACAAGGCTTTGGGATTC-3′). Amplification reactions were performed in a solution (50 μl) containing 20 pmol each of the appropriate primer, ~1 μg of genomic DNA, 5 μl of 10× polymerase chain reaction (PCR) buffer, 0.2 μM deoxynucleotide triphosphate, and 1 unit of Taq polymerase (Boehringer Mannheim, Meylan, France). The PCR cycling conditions were 95°C for 5 min followed by 30 cycles of 95°C for 1 min, 52°C for 1 min, and 72°C for 1 min and ended by 10 min at 72°C. SSCP: two amplification reactions performed under the conditions described above used the primers V1 forward and V5 reverse to amplify the totality of the CX_3CR1 open reading frame. Five fluorescent pairs were used to generate five overlapping segments of 200- to 350-bp DNA fragments: V1 forward and V1 reverse (5′-GGAGGCCCTTTTCATTTATCA-3′), V2 forward (5′-AACAGCAAGAAGCCCAAGAGT-3′) and V2 reverse (5′-CGCCTAGGCT GATGGTGAC-3′), V3 forward (5′-GCCGCCAACTCCATGAAC-3′) and V3 reverse (5′-CAGGAAAACAGCGTCTGGAT-3′), V4 forward (5′-GAGGTCCTCCAGGAAATC TGGCCCGTG-3′) and V4 reverse (5′-GGCCAGCCTCAGATCCT-TCTT-3′), V5 forward (5′-CTCTATGACTTCTTTC-CCAGTTGT-3′) and V5 reverse. The amplification products were diluted in a formamide solution, denatured at 95°C for 5 min, and loaded on mutation detection gel solution from FMC Bioproducts. Gels were run on an ABI PRISM 377 DNA sequencer (Perkin-Elmer, Courtaboeuf, France) under the following conditions: filter C, 30°C, 4000 V, 60 mA, 60 W, 18 hours. The results were analyzed with Genotyper software.
19. M. Magierowska *et al.*, *Microbes Infect.* **2**, 123 (1999).
20. Amplification reactions were performed with the following primers: V4 forward and V5 reverse under the same conditions as the initial amplification reaction. The amplification products were digested 2 hours at 55°C with the *Bsm* BI enzyme (New England Biolabs, Ozyme, Saint Quentin en Yvelines, France) and 2 hours at 37°C with *Psp* 1406 I (Boehringer Mannheim, Meylan, France), which, respectively, allow detection of mutations V249I and T280M.
21. M. Magierowska *et al.*, *Blood* **93**, 936 (1999); L. Meyer *et al.*, *AIDS* **11**, F73 (1997); I. Theodorou, L. Meyer, M. Magierowska, C. Katlama, C. Rouzioux, *Lancet* **349**, 1219 (1997). Only French Caucasian subjects were studied: 63 were from the ALT cohort, 73 were from the IMMUNOCO cohort, 426 were from the SEROCO cohort, and 78 were uninfected blood donors. Human genomic DNA was purified from whole blood with a DNA purification kit (QIAamp DNA Blood minikit, Qiagen, Courtaboeuf, France).
22. Haplotypes were inferred from two observations. First, all individuals homozygous for M280 were also homozygous for I249; second, when cloned products from 10 M280 heterozygous individuals were being sequenced, the chromosome bearing M280 was always bearing I at position 249. Haplotype frequencies were derived from genotypes using the EM algorithm as implemented in the EH program; X. Xie *et al.*, *Am. J. Hum. Genet. Suppl.* **53**, 1107 (1993). The likelihood ratio test for linkage disequilibrium was done with this same program.
23. Hardy-Weinberg proportions were tested with a χ^2 test or an exact test when sample size were too small: S. Guo and E. Thompson, *Biometrics* **48**, 361 (1992).
24. We performed a case-control analysis, defining cases as subjects in the ALT cohort and controls as subjects in the IMMUNOCO cohort. Cases and controls were compared for baseline characteristics with the χ^2 test. A multivariate logistic regression was used to assess the roles of the CX_3CR1 genotypes, taking into account age and presence of the CCR5-Δ32 deletion. AIDS-free survival curves (1993 European definition) for SEROCO patients were constructed by the Kaplan-Meier method and compared with the log-rank test. Crude and adjusted RR values were calculated with Cox proportional hazards models.
25. Data not shown.
26. M. Parmentier and A. Maho, personal communication.
27. S. Mummidi *et al.*, *Nat. Med.* **4**, 786 (1998).
28. Binding experiments were done with ^{125}I-labeled fractalkine (specific activity 2200 Ci per millimole of protein) purchased from Amersham (Saclay, France). After washing in PBMCs, 3×10^5 cells were incubated in duplicate with increasing amounts of ^{125}I-labeled fractalkine in the presence or absence of a 500-fold excess of unlabeled recombinant human fractalkine (R & D Systems, Abingdon Oxon, UK) in binding medium [Hanks' balanced salt solution (HBSS) with 1 mg of bovine serum albumin (BSA) per milliliter and 0.01% azide, pH 7.4] in a total volume of 200 μl. After incubation for 2 hours at room temperature, unbound chemokine was separated from cells by washing with 1 ml of HBSS containing 0.5 M NaCl, BSA at 1 mg/ml, and 0.01% azide. γ emissions in the cell pellet were then assayed.
29. J. He *et al.*, *Nature* **385**, 645 (1997).

30. Supported by grants from the Agence Nationale de Recherches sur le SIDA and from SIDACTION. We thank P. Deterre, F. C. Darpoux, and P. A. Zimmerman for their helpful discussions.

24 September 1999; accepted 10 February 2000